American Journal of Transplantation 25 (2025) 72–87

Contents lists available at ScienceDirect

American Journal of Transplantation

journal homepage: www.amjtransplant.org

Original Article

Subthreshold rejection activity in many kidney transplants currently classified as having no rejection

Philip F. Halloran [1,*,†], Katelynn S. Madill-Thomsen [2,†], Georg Böhmig [3], Jonathan Bromberg [4], Klemens Budde [5], Meagan Barner [6], Martina Mackova [2], Jessica Chang [2], Gunilla Einecke [7], Farsad Eskandary [3], Gaurav Gupta [8], Marek Myślak [9], Ondrej Viklicky [10], Enver Akalin [11], Tarek Alhamad [12], Sanjiv Anand [13], Miha Arnol [14], Rajendra Baliga [15], Mirosław Banasik [16], Adam Bingaman [17], Christopher D. Blosser [18], Daniel Brennan [19], Andrzej Chamienia [20], Kevin Chow [21], Michał Ciszek [22], Declan de Freitas [23], Dominika Dęborska-Materkowska [24], Alicja Debska-Ślizień [25], Arjang Djamali [26], Leszek Domański [27], Magdalena Durlik [28], Richard Fatica [29], Iman Francis [30], Justyna Fryc [31], John Gill [32], Jagbir Gill [32], Maciej Glyda [33], Sita Gourishankar [1], Ryszard Grenda [34], Marta Gryczman [35], Petra Hruba [36], Peter Hughes [21], Arskarapurk Jittirat [37], Zeljka Jurekovic [38], Layla Kamal [39], Mahmoud Kamel [15], Sam Kant [40], Bertram Kasiske [41], Nika Kojc [42], Joanna Konopa [20], James Lan [32], Roslyn Mannon [43], Arthur Matas [44], Joanna Mazurkiewicz [45], Marius Miglinas [46], Thomas Müller [47], Seth Narins [48], Beata Naumnik [31], Anita Patel [30], Agnieszka Perkowska-Ptasińska [24], Michael Picton [49], Grzegorz Piecha [50], Emilio Poggio [51], Silvie Rajnochová Bloudíčkova [52], Milagros Samaniego-Picota [53], Thomas Schachtner [54], Sung Shin [55], Soroush Shojai [56], Majid L.N. Sikosana [1], Janka Slatinská [36], Katarzyna Smykal-Jankowiak [33], Ashish Solanki [57], Željka Veceric Haler [14], Ksenija Vucur [58], Matthew R. Weir [59], Andrzej Wiecek [50], Zbigniew Włodarczyk [60], Harold Yang [61], Ziad Zaky [62]

Abbreviations: AA, archetypal analysis; ABMR, antibody-mediated rejection; ATAGC, Alberta Transplant Applied Genomics Centre; dd-cfDNA, donor-derived cell-free DNA; DSA, donor-specific antibody; EABMR, early-stage antibody-mediated rejection; eGFR, estimated glomerular filtration rate; FABMR, fully developed antibody-mediated rejection; INTERCOMEX, International Collaborative Microarray Extension Study; LABMR, late-stage antibody-mediated rejection; MMDx, Molecular Microscope Diagnostic System; NR, No rejection; PCA, principal component analysis; PC, principal component; TCMR, T cell–mediated rejection; TG, transplant glomerulopathy; UMAP, uniform manifold approximation and projection.

* Corresponding author. Alberta Transplant Applied Genomics Centre, #250 Heritage Medical Research Centre, University of Alberta, Edmonton, AB T6G 2S2, Canada.

† These authors are cofirst authors: Philip F. Halloran and Katelynn S. Madill-Thomsen.

https://doi.org/10.1016/j.ajt.2024.07.034

Received 8 May 2024; Received in revised form 19 June 2024; Accepted 31 July 2024

Available online 6 August 2024

[1] Department of Medicine, Division of Nephrology & Transplantation Immunology, University of Alberta, Canada
[2] Alberta Transplant Applied Genomics Centre, Canada
[3] Division of Nephrology and Dialysis, Department of Medicine III, Medical University of Vienna, Austria
[4] Department of Surgery, University of Maryland, USA
[5] Department of Nephrology, Charite-Medical University of Berlin, Germany
[6] Kashi Clinical Laboratories, USA
[7] Department of Nephrology, Medical University of Hannover, Germany
[8] Department of Internal Medicine, Division of Nephrology, Virginia Commonwealth University, USA
[9] Department of Clinical Interventions, Department of Nephrology and Kidney Transplantation SPWSZ Hospital, Pomeranian Medical University, Poland
[10] Department of Nephrology and Transplant Center, Institute for Experimental and Clinical Medicine, Czech Republic
[11] Albert Einstein College of Medicine, Montefiore Medical Center, USA
[12] Division of Nephrology, Washington University at St. Louis, USA
[13] Intermountain Transplant Services, USA
[14] Department of Nephrology, University of Ljubljana, Slovenia
[15] Tampa General Hospital, USA
[16] Department of Nephrology and Transplantation Medicine, Medical University of Wrocław, Poland
[17] Department of Surgery, Methodist Transplant and Specialty Hospital, USA
[18] University of Washington, USA
[19] Department of Medicine, Johns Hopkins University School of Medicine, USA
[20] Department of Nephrology, Transplantology and Internal Diseases, Medical University of Gdańsk, Poland
[21] Department of Nephrology, The Royal Melbourne Hospital, Australia
[22] Department of Immunology, Transplantology and Internal Diseases, Warsaw Medical University, Poland
[23] Department of Renal Research, Manchester Royal Infirmary, United Kingdom
[24] Department of Transplantation Medicine, Warsaw Medical University, Poland
[25] Department of Nephrology, Transplantology and Internal Medicine, Medical University of Gdańsk, Poland
[26] Department of Medicine, University of Wisconsin, USA
[27] Department of Nephrology, Transplantology and Internal Medicine, Pomeranian Medical University, Poland
[28] Department of Transplantology, Immunology, Nephrology and Internal Diseases, Warsaw Medical University, Poland
[29] Department of Kidney Medicine, Cleveland Clinic Foundation, USA
[30] Henry Ford Transplant Institute, USA
[31] 1st Department of Nephrology and Transplantation With Dialysis Unit, Medical University in Bialystok, Poland
[32] St. Paul's Hospital, Canada
[33] Wojewodzki Hospital, Poland
[34] Department of Nephrology, Kidney Transplantation and Hypertension, The Children's Memorial Health Institute, Poland
[35] Department of Nephrology and Kidney Transplantation, Pomeranian Medical University, Poland
[36] Department of Nephrology, Institute for Experimental and Clinical Medicine, Czech Republic
[37] University Hospital Cleveland Medical Center, USA
[38] Renal Replacement Therapy, Department of Nephrology, University Hospital Merkur, Croatia
[39] Division of Nephrology, Department of Medicine, Virginia Commonwealth University, USA
[40] Division of Nephrology & Comprehensive Transplant Center, Department of Medicine, Johns Hopkins University School of Medicine, USA
[41] Department of Medicine, Hennepin County Medical Centre, USA
[42] Department of Pathology, University of Ljubljana, Slovenia
[43] Division of Nephrology, Department of Medicine, University of Alabama at Birmingham, USA
[44] Department of Surgery, Division of Transplantation, University on Minnesota, USA
[45] Pomeranian Medical University, Poland
[46] Nephrology and Kidney Transplantation Unit, Nephrology Center, Vilnius University Hospital Santaros Klinikos, Lithuania
[47] Nephrology Department, University Hospital Zurich, Switzerland
[48] PinnacleHealth Transplant Associates, USA
[49] Department of Renal Medicine, Manchester Royal Infirmary, United Kingdom
[50] Department of Nephrology, Transplantation and Internal Medicine, Silesian Medical University, Poland
[51] Department of Kidney Medicine, Glickman Urological and Kidney Institute, Cleveland Clinic Foundation, USA
[52] Department of Nephrology, Transplant Center, Institute for Experimental and Clinical Medicine, Czech Republic
[53] Division of Nephrology, University of Michigan, USA
[54] Department of Surgery and Transplantation, University Hospital Zurich, Switzerland
[55] Department of Laboratory Medicine, University of Ulsan College of Medicine/Assan Medical Center, South Korea
[56] Division of Nephrology, Department of Medicine, University of Alberta, USA
[57] Johns Hopkins University School of Medicine, USA
[58] Department of Nephrology, University Hospital Merkur, Croatia
[59] Department of Medicine, Division of Nephrology, University of Maryland, USA
[60] University Hospital no. 1, Poland
[61] Department of Surgery, PinnacleHealth Transplant Associates, USA
[62] Cleveland Clinic Foundation, USA

ARTICLE INFO

Keywords:
kidney transplant
biopsy
microarray
transplant rejection
ABMR
TCMR
gene expression
gradients

ABSTRACT

Most kidney transplant patients who undergo biopsies are classified as having no rejection based on consensus thresholds. However, we hypothesized that because these patients have normal adaptive immune systems, T cell–mediated rejection (TCMR) and antibody-mediated rejection (ABMR) may exist as subthreshold activity in some transplants currently classified as no rejection. To examine this question, we studied genome-wide microarray results from 5086 kidney transplant biopsies (from 4170 patients). An updated molecular archetypal analysis designated 56% of biopsies as no rejection. Subthreshold molecular TCMR and/or ABMR activity molecular activity was detectable as elevated classifier scores in many biopsies classified as no rejection, with ABMR activity in many TCMR biopsies and TCMR activity in many ABMR biopsies. In biopsies classified as no rejection histologically and molecularly, molecular TCMR classifier scores correlated with increases in histologic TCMR features and molecular injury, lower estimated glomerular filtration rate, and higher risk of graft loss, and molecular ABMR activity correlated with increased glomerulitis and donor-specific antibody. No rejection biopsies with high subthreshold TCMR or ABMR activity had a higher probability of having TCMR or ABMR, respectively, diagnosed in a future biopsy. We conclude that many kidney transplant recipients have unrecognized subthreshold TCMR or ABMR activity, with significant implications for future problems.

1. Introduction

Following the introduction of organ transplantation in 1954,[1] the development of effective immunosuppressive drug (ISD) protocols made transplants an essential element in managing end-stage organ failure, creating a large population of functioning grafts requiring long-term management. Organ transplant patients have normal adaptive immune systems, and all are at risk for T cell–mediated rejection (TCMR) and antibody-mediated rejection (ABMR) and must be maintained indefinitely on ISDs to prevent rejection.[2,3] Rejection is diagnosed by assessing biopsies triggered by indications such as dysfunction and usually interpreted by histology following Banff guidelines,[4] or by noninvasive screening tests such as measurement of donor-specific antibodies (DSAs)[5,6] and donor-derived cell-free DNA (dd-cfDNA).[7]

Recently, molecular biopsy phenotyping has offered an additional dimension for biopsy assessment. We developed the Molecular Microscope Diagnostic System (MMDx) to characterize the molecular phenotypes of biopsies.[8,9] MMDx measures gene expression using genome-wide microarrays and interprets disease states such as injury,[10] TCMR,[11] and ABMR[12,13] using ensembles of machine learning algorithms. Molecular assessment of kidney transplant biopsies discovered that many biopsies classified as no rejection had subtle molecular ABMR activity.[14,15] This raised the possibility that there were also subtle gradients of TCMR activity among NR biopsies. Indeed, because all patients are capable of cognate T cell and B cell immune responses against graft alloantigens, ISDs may only be controlling the upper end of rejection activity, permitting smoldering cognate immune responses in many patients.

In the present study, we hypothesized that TCMR and ABMR operate as continuous gradients rather than dichotomous classes, with subthreshold ABMR and/or TCMR activity in many biopsies called no rejection and with unrecognized ABMR activity in TCMR and TCMR activity in ABMR. To address this issue, we aimed to increase the power of the molecular classification algorithms by expanding the number of molecularly phenotyped biopsies available for training the algorithms to 5086 by combining 3570 biopsies collected during clinical trials with 1516 anonymized service biopsies (Fig. 1A, B). This was possible because the MMDx is standardized with identical technology and algorithms in the research laboratory (ATAGC) and the service laboratory (Kashi Clinical Laboratories). New molecular algorithms were developed in the combined cohort and tested for their relationships to the histology lesions, function, and outcomes in the fully phenotyped ClinicalTrials.gov biopsies. We were particularly interested in how the new, more rigorous classification of rejection would impact the assessment of subthreshold rejection activity in biopsies considered to have no rejection, and aimed to define the extent and clinical significance of subthreshold molecular TCMR and ABMR activity.

2. Materials and methods

2.1. Study population and data collection

The new cohort of biopsies included 3570 biopsies from the prospective MMDx-Kidney studies (International Collaborative Microarray Extension Study [INTERCOMEX], NCT01299168, and Trifecta, NCT04239703). Study workflow and biopsy inclusion are shown in Figure 1A-B. As approved by institutional review boards, phenotype data were collected by the local centers for the ClinicalTrials.gov biopsies.[16-23] We added 1516 biopsies processed in

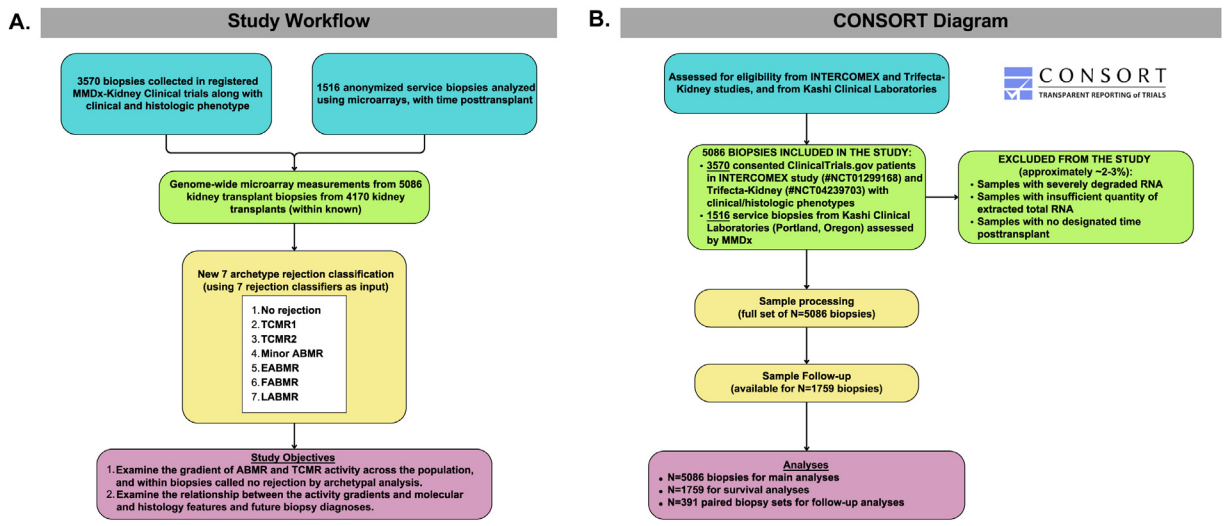

Figure 1. (A) Study design and (B) CONSORT diagram showing biopsy inclusion. Biopsies were pooled from the INTERCOMEX study, Trifecta-Kidney study, and anonymized service biopsies from the Kashi Clinical Laboratories to create the 5086 data set.

the Kashi service laboratory, for which minimal phenotype data were available. Demographics and further details for biopsies with available data are shown in Supplementary Table S1.

2.2. Biopsy processing

As previously described,[8] a portion of 1 core of each biopsy (mean length 3 mm)[19] was immediately stabilized in RNA*later* and shipped at ambient temperature to ATAGC (http://atagc.med.ualberta.ca) or Kashi Clinical Laboratories for RNA extraction and processing.[19] Gene expression was measured using Affymetrix PrimeView microarrays. Molecular diagnoses were made independently of the biopsy's histology, clinical data, and human leukocyte antigen antibody status. MMDx reports were sent to the participating centers from ATAGC or from Kashi Clinical Laboratories, usually within 2 working days of receiving the biopsy.

2.3. Pathogenesis-based transcript sets

Pathogenesis-based transcript sets used throughout these analyses are detailed in Supplementary Table S2.

2.4. Updating the published classifiers

As in earlier analyses, 7 base rejection classifiers were used to build the new principal component analysis (PCA) and archetypal analysis (AA), based on probabilities of histologic ABMR/TCMR diagnosis, or lesion scores ($ABMR_{Prob}$, $TCMR_{Prob}$, $g>0_{Prob}$, $ptc>0_{Prob}$, $cg>0_{Prob}$, $i>1_{Prob}$, and $t>1_{Prob}$). AA and PCA used published methods[20] and were updated using the 5086 biopsy data set. Classifier development methodology is described in Supplementary Figure S1 using the $ABMR_{Prob}$ classifier as an example.

2.5. AA and PCA

The rejection-based PCA and AA were updated to the 5086-biopsy cohort using the matrix of 5086 (biopsies) by 7 (base classifier scores) inputs. We selected a 7-archetype model (rather than 6 as in previous publications[14]) to capture minor rejection below the lower boundaries of the previous classes. Each biopsy gets 7 archetype scores (summing to 1.0), and the highest score determines the archetype cluster to which the biopsy is assigned.

2.6. Statistical analysis

All analyses were performed in the R computing language version 4.1.1.2.[24]

3. Results

3.1. Patient and biopsy characteristics

The cohort included 5086 biopsies from 4170 patients; 71% of kidney grafts were from deceased donors (Supplementary Table S1). Of biopsies with available data, 82% were for indications. Among kidneys with available follow-up (mean follow-up time in functioning grafts = 728 days), 300 kidneys (20%) failed and 1213 (80%) were functioning (censored). In addition to automated archetype assignments, all biopsies were signed out in an MMDx report as TCMR, ABMR, Mixed rejection, possible TCMR or ABMR, or No rejection. Thus, 3 definitions of rejection were available: automatically assigned archetypes, MMDx report signouts, and histology.

3.2. Developing a new archetypal classification of rejection

All classifiers were rederived in the expanded 5086 biopsy population as ensembles of 12 machine learning programs and cross-validated. Supplementary Table S3 summarizes the features on which the classifiers were trained and the areas under the curve (AUCs) for the prediction of these training features in the test sets for each classifier. The AUCs ranged from AUC = 0.80 ($cg>0_{Prob}$) to 0.85 ($Rejection_{Prob}$). Note that the purpose of

these classifiers is to identify and quantify the underlying molecular states associated with these features, not to predict the training feature.

Supplementary Figure S2 shows the relationship between the time of biopsy posttransplant and the rejection classifier scores in the 5086 cohort, represented as smoothed curves (splines). TCMR-related classifier scores peaked between 1 and 2 years and then fell progressively after 3 years. ABMR-related classifier scores rose more slowly and were the dominant scores after 3 years. The $cg>0_{Prob}$ classifier score increased after 3000 days posttransplant because cg-lesions reflect a more advanced ABMR stage.

The molecular classifier scores assigned to all 5086 biopsies by the updated classifiers were used to create a new archetype classification, which gave each biopsy 7 archetype scores. Each biopsy was assigned to an archetype group based on its highest archetype score. We chose a 7-archetype model rather than the previous 6-archetype model to capture more biopsies with rejection and reduce the number of biopsies called archetypal No rejection (NR). Groups are named for their molecular and histologic features as follows: NR, TCMR1, TCMR2, Minor ABMR, early-stage antibody-mediated rejection (EABMR), fully-developed antibody-mediated rejection (FABMR), and late-stage antibody-mediated rejection (LABMR).

Figure 2A, B shows all 5086 biopsies distributed in PCA (using rejection classifier scores as input) and colored by their archetype group. In Figure 2A, principal component (PC) 1 separated NR from all rejection and PC2 separated TCMR (negative) from ABMR (positive). In Figure 2B, PC3 separated ABMR into EABMR, FABMR, and LABMR, similar to earlier classifications.[14,20] However, the new classification also recognized some biopsies with Minor ABMR near the boundary with NR, compatible with a less active or transitional ABMR state.

Figure 2C uses uniform manifold approximation and projection (UMAP) to visualize the biopsy population, compressing all variance into 2 dimensions. The new group of Minor ABMR biopsies inhabits a region intermediate between the NR and the EABMR, FABMR, and LABMR archetypes.

For visualization purposes, we drew an approximate boundary (solid black line, Fig. 2C) to roughly separate plotted regions with biopsies called ABMR (blue, purple, cyan, orange) from those called NR (gray), ABMR from TCMR (red, green), and any rejection (ABMR plus TCMR) from NR. We note that rejection activity in PCA and UMAP operates as continuous distributions and does not separate into distinct groups.

3.3. Details of the archetype groups

As expected, the rejection archetype groups were strongly related to rejection-related molecular and histologic features (Figure 2D-G and Supplementary Table S3). TCMR1 and TCMR2 biopsies had increased scores for the 3 TCMR-related classifiers ($TCMR_{Prob}$, $i>1_{Prob}$, and $t>1_{Prob}$, Fig. 2D) and for histologic i- and t-lesions (Fig. 2E). Histologic v-lesions occurred mainly in TCMR1 but also in TCMR2, EABMR, and FABMR (Fig. 2E). The ABMR archetypes had increased scores for ABMR activity-related molecular classifiers ($ABMR_{Prob}$, $ptc>1_{Prob}$, and $g>0_{Prob}$, Fig. 2F) and histologic g- and ptc-lesions (Fig. 2G). These scores were not only highest in FABMR but also prominent in EABMR. All ABMR molecular scores were mildly increased in Minor ABMR. TCMR1 also had increased ABMR molecular scores and histologic activity, that is, ptc- and g-lesions but not cg-lesions, indicating that TCMR1 often has EABMR. The main features of the new Minor ABMR group included an increased level of DSA-specific and ABMR-specific histologic lesions and molecular activity compared with biopsies called NR, but less than in the EABMR, FABMR, or LABMR groups.

Scores for the ABMR activity classifiers and lesions generally increased from Minor ABMR to EABMR to FABMR, then declined in LABMR. The $cg>0_{Prob}$ classifier (Fig. 2F) and cg-lesion scores (Fig. 2G) were increased in FABMR and LABMR as expected because the cg-lesion is a time-dependent ABMR stage feature. DSA positivity (Fig. 2G) was increased in all ABMR groups, maximal in FABMR. ABMR had mildly increased mean i-lesion scores as previously reported.[13]

The archetypes represent the dominant molecular process in a biopsy and do not specifically designate "mixed rejection." However, TCMR1 often had molecular and histologic ABMR features and increased DSA-positivity (51%), and MMDx signouts designated 66% of TCMR1 biopsies as mixed rejection. Supplementary Table S4 provides further details of each rejection archetype group.

Figure 3 shows how the number and relative frequency of biopsies assigned to each archetype varies with time posttransplant. Figure 3A shows smoothed densities for the numbers of biopsies within each archetype class over time; Figure 3B removes NR biopsies to better visualize the detail in rejection groups. Figure 3C shows the proportion of biopsies within each archetype class over time, and Figure 3D removes NR. Most early biopsies were NR, with some EABMR, presumably reflecting pre-sensitization. The frequency of TCMR1 and TCMR2 biopsies peaked between 300 and 1000 days then both steadily declined. FABMR biopsies became the dominant archetype after 1000 days, with LABMR biopsies increasing after 3000 days. Minor ABMR was not closely related to time.

Injury-related features of the rejection archetypes are shown in Supplementary Table S5. Compared with NR, TCMR1 and TCMR2 showed extensive injury as measured by the recent injury-induced transcripts[25] and depression of estimated glomerular filtration rate (eGFR). TCMR2 had elevated atrophy fibrosis as previously reported.[11] ABMR archetype groups had less injury and higher eGFR than TCMR, but there was a progression of injury from EABMR to FABMR to LABMR.

Kaplan-Meier estimates of death-censored 3-year survival postbiopsy were higher in NR (80%) and Minor ABMR (93%) and lower in TCMR1 (63%), TCMR2 (63%), FABMR (59%), and LABMR (57%) (Supplementary Table S5, Fig. 3E, using 1 random biopsy per patient). EABMR was well-tolerated until approximately 2 years postbiopsy before the probability of failure increased; 3-year survival was estimated at 0.74. (Note that

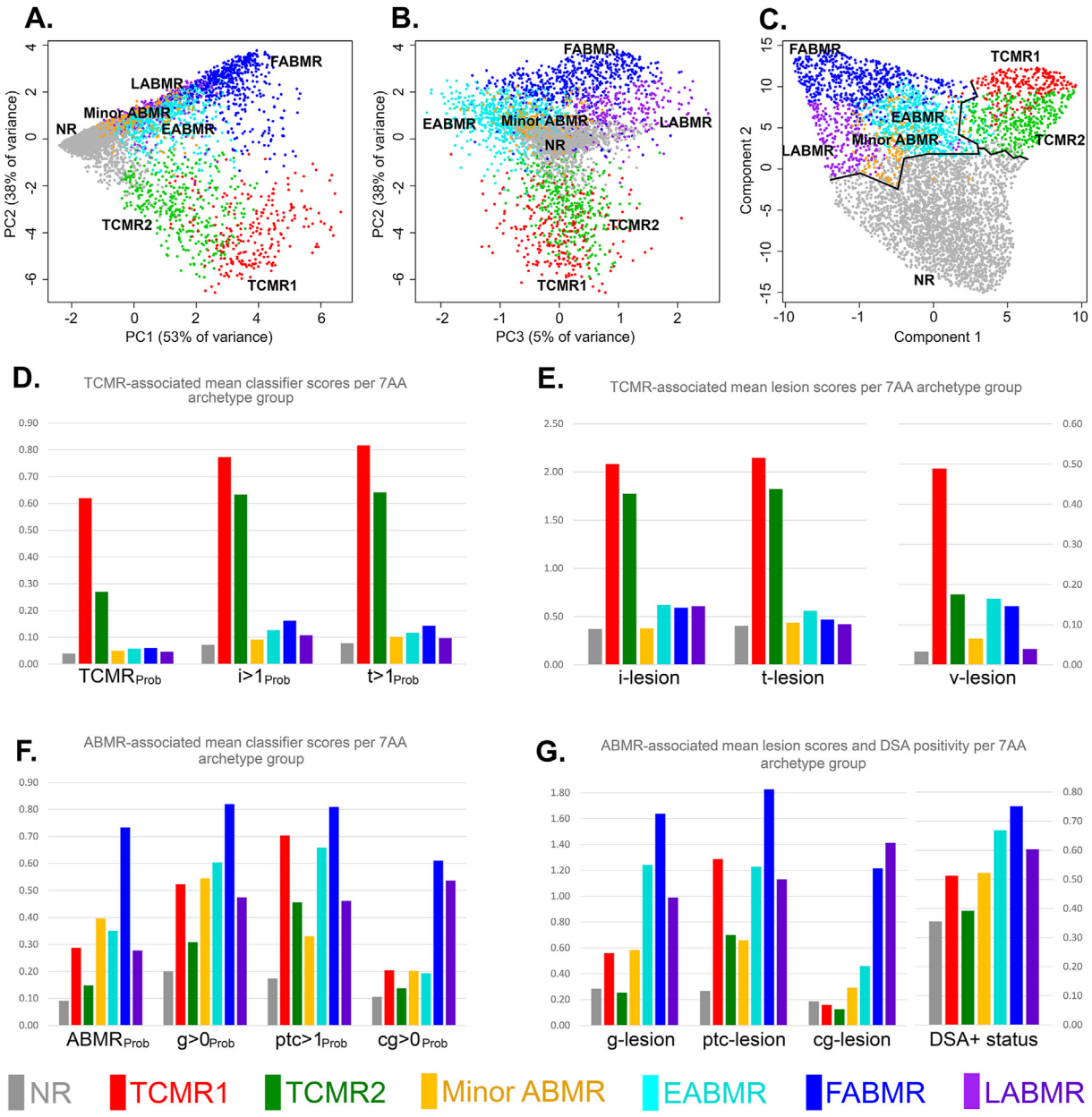

Figure 2. Principal component analysis (PCA) and uniform manifold approximation and projection (UMAP) visualizations of the 5086 kidney transplant biopsy population: (A) principal component (PC) 2 vs PC1, (B) PC2 vs PC3, and (C) UMAP visualizations colored by the 7-archetype rejection model cluster assignments (No rejection "NR," TCMR1, TCMR2, EABMR, FABMR, LABMR, and Minor ABMR). The black line in the UMAP plot in (C) illustrates the approximate boundary between no rejection and rejection (ABMR and/or TCMR) archetype groups. Bar plots showing the mean scores for selected (D, E) TCMR-associated and (F, G) ABMR-associated features, bars colored according to archetype groups. DSA status on (G) is reported as values 1 (positive) or 0 (negative) and the mean displayed on the plot. ABMR, antibody-mediated rejection; DSA, donor-specific antibody; TCMR, T cell–mediated rejection.

these survival results in the biopsied population [most for indications] are lower than survival recorded in registry populations.)

3.4. Gradients in rejection-related activity

The updated rejection classifiers were used to examine the rejection activity gradients in the 5086 biopsy cohort. We defined all-rejection activity by the $Rejection_{Prob}$ score, ABMR activity by the $ABMR_{Prob}$ score, and TCMR activity by the $TCMR_{Prob}$ score.

Figure 4 visualizes the gradients using the same UMAP plots as Figure 2C. All-rejection activity ($Rejection_{Prob}$) formed a vertical gradient with considerable activity in NR biopsies (Fig. 4A). ABMR activity ($ABMR_{Prob}$) peaked at the upper left (FABMR region) but extended into TCMR and NR (Fig. 4B). TCMR activity ($TCMR_{Prob}$) peaked at the upper right (TCMR1 region) and extended into ABMR and NR (Fig. 4C).

Figure 4D-F shows the same gradients calibrated by dividing the scores into quintiles to more equally represent the actual scores. The lower 3 quintiles were located primarily within NR

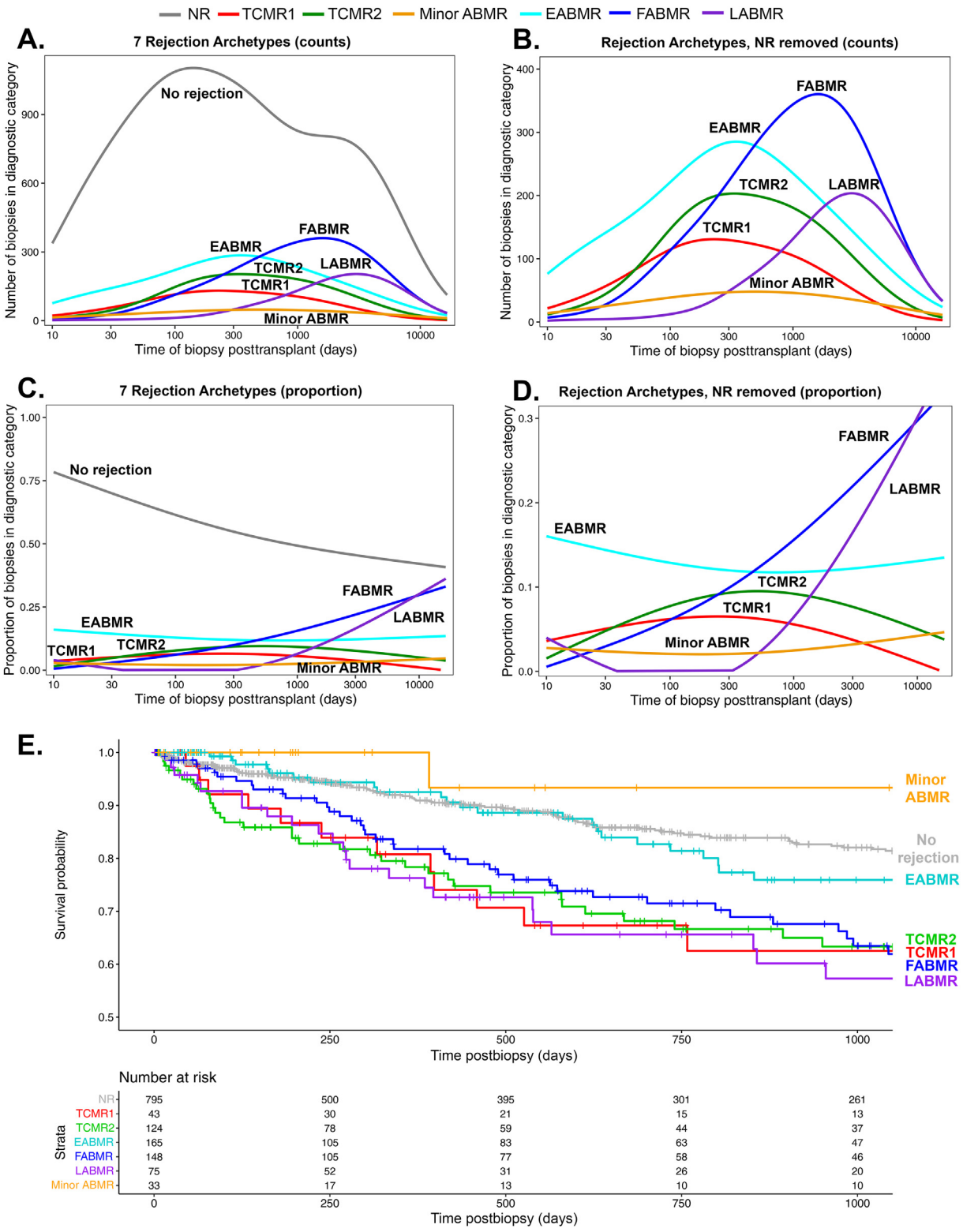

(caption on next page)

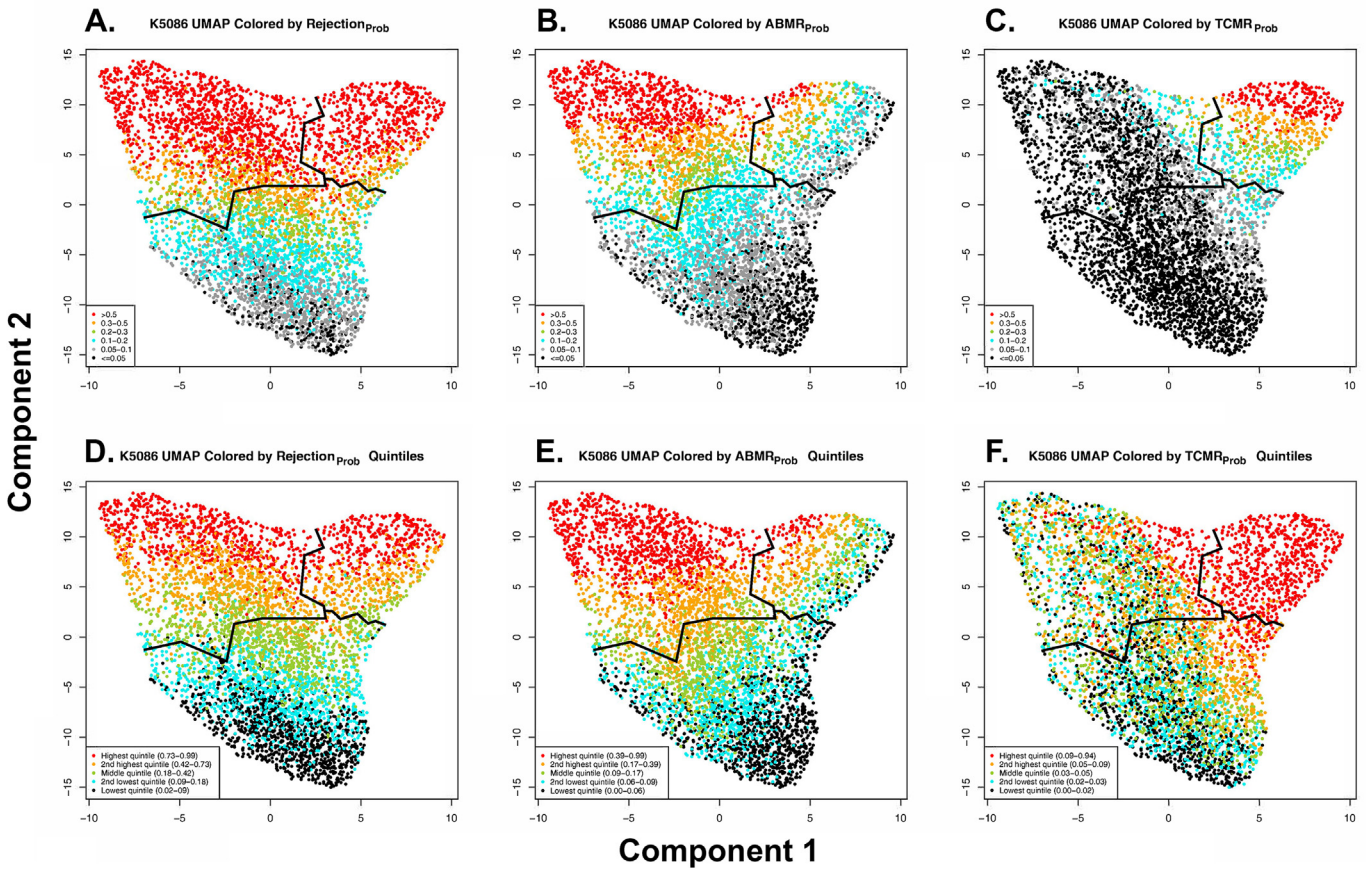

Figure 4. UMAP visualizations of the 5086 kidney transplant population, showing the gradient across the population of various selected molecular scores, colored according to various score cutoffs with red highest and black lowest. The thin black line is the same boundary introduced in Figure 3 to separate NR from all rejection and shows the approximate boundary between No rejection, the ABMR, and the TCMR archetype groups. Using arbitrarily selected cutoffs, the UMAPs colored according to the (A) Rejection$_{Prob}$, (B) ABMR$_{Prob}$, and (C) TCMR$_{Prob}$ classifier scores. (D-F) Biopsies colored by quintiles of the same scores as in A-C, with the whole population divided into 5 equal groups. ABMR, antibody-mediated rejection; NR, No rejection; TCMR, T cell–mediated rejection; UMAP, uniform manifold approximation and projection.

biopsies, revealing subthreshold molecular rejection in many biopsies classified as NR by archetypes. This is particularly evident for biopsies with TCMR scores of <0.05 (colored black in Fig. 4C), which have extensive middle (green) and second-lowest (cyan) quintiles of TCMR activity within NR and ABMR biopsies (Fig. 4F). This is of interest because we previously considered TCMR scores of <0.05 to be negative.

Figure 5 visualizes gradients for other molecular scores. In Figures 5A-B, the gradients for the ABMR-related ptc>0$_{Prob}$ and g>0$_{Prob}$ classifiers extend into the TCMR region (particularly the ptc>0$_{Prob}$ classifier) and the NR region. The cg>0$_{Prob}$ gradient (Fig. 5C) was more biased toward the ABMR area, as expected because the cg-lesions reflect a later ABMR stage (FABMR and LABMR). In Figures 5D-E, the gradients for TCMR-related i>1$_{Prob}$ and t>1$_{Prob}$ classifier scores are similar to the TCMR$_{Prob}$ score gradient.

Figure 5F examines the gradient of recent molecular injury, represented by the acute kidney injury-induced injury-repair

Figure 3. Time course visualizations and survival by rejection archetype groups. The probability that a biopsy at any given time point posttransplant will be assigned to each archetype group was represented by conditional probability plots and cubic splines (knots = 3). Density estimates, and subsequent conditional probability estimates, were calculated using the "density" function in the R package 'stats'.[24] Splines for conditional probabilities over time posttransplant were restricted cubic splines generated using the R package 'mgcv'.[37] Splines representing classifiers over time posttransplant were restricted cubic splines generated using the R package 'rms'.[38] (A) Density plot showing the estimated distribution of biopsies in each archetype category over time posttransplant. (B) Same results as (A), but with NR biopsies removed for closer examination of the rejection curves. (C) Conditional probability plot showing the estimated proportion of biopsies in each archetype category over time posttransplant. (D) Same results as (C) but with NR biopsies removed for closer examination of the rejection curves. (E) Three-year survival analyses in the 5086 kidney transplant population assessed using Kaplan-Meier curves, each line representing an archetype group, 1 random biopsy per patient (n = 1292, 210 failures). Minor ABMR has the best overall survival (although relatively low N) over 3 y posttransplant, followed by NR. TCMR2, TCMR1, and LABMR have the lowest survival. ABMR, antibody-mediated rejection; DSA, donor-specific antibody; EABMR, early-stage antibody-mediated rejection; FABMR, fully-developed antibody-mediated rejection; LABMR, late-stage antibody-mediated rejection; NR, No rejection; TCMR, T cell–mediated rejection.

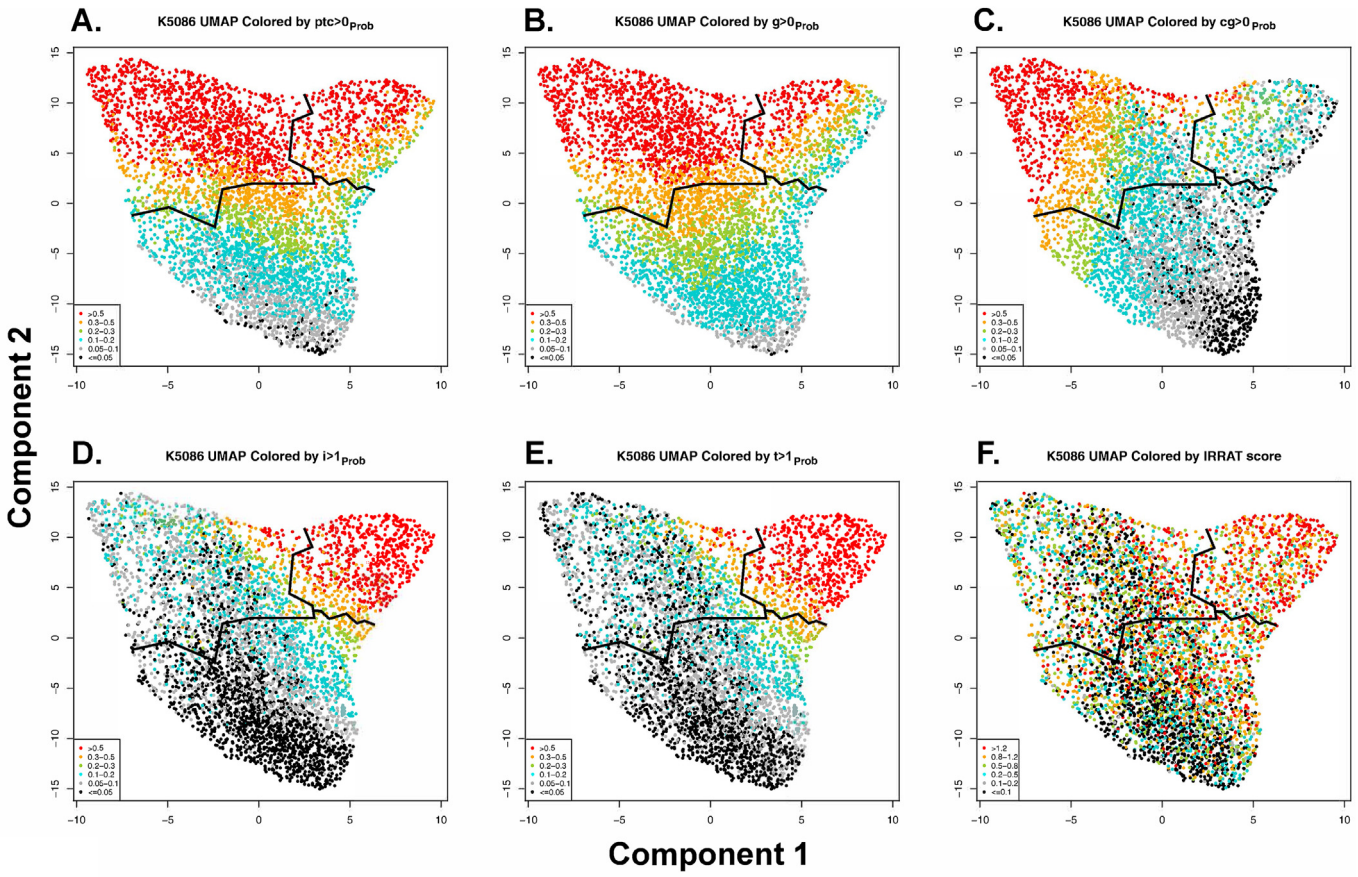

Figure 5. UMAP visualizations of the 5086 kidney transplant population colored by various cut-offs selected for 3 ABMR-related classifier scores: (A) ptc>0_{Prob} score, (B) g>0_{Prob} score, and (C) the cg>0_{Prob} score. The UMAP was also colored by 2 TCMR-related classifier scores: (D) the i>1_{Prob} score and (E) t>1_{Prob} score, as well as the (F) recent injury score (IRRAT score). Highest scores are colored red, and lowest scores colored black. The thin black line is the same boundary introduced in Figure 3 to separate NR from all rejection and shows the approximate boundary between NR, ABMR, and TCMR archetype groups. ABMR, antibody-mediated rejection; NR, No rejection; TCMR, T cell–mediated rejection; UMAP, uniform manifold approximation and projection.

response-associated (IRRAT) transcript set score.[25] Injury was distributed in many regions, but virtually all TCMR biopsies had extensive injury (red or orange symbols). Severe injury was less common in ABMR.

3.5. Correlation of ABMR and TCMR activity with histologic and clinical features in NR biopsies

We considered the possibility that, at the low end, the ABMR and TCMR classifiers were simply nonspecific. If so, low-level activity would not be associated with the conventional features selective for ABMR and TCMR, respectively. We examined Spearman correlations between rejection-associated classifier scores and conventional features using all biopsies and in biopsies classified as no rejection, defined by 3 different levels of stringency. Level 1 was 2843 biopsies assigned to the NR archetype group. Level 2 required that, in addition to being assigned to the NR archetype, the MMDx signout must be no rejection and/or no possible rejection, yielding 2341 biopsies. Level 3 required Level 2 criteria plus histologic assessment of no rejection; 715 biopsies met Level 3 criteria for no molecular or histologic rejection or possible rejection. (There were fewer biopsies in this group in part because histologic assessment was not available for anonymized service laboratory biopsies.)

In all biopsies, as expected, TCMR activity (Table 1) correlated strongly with i-, t-, and v-lesions and less strongly with ptc-lesions; with high molecular injury scores, low eGFR, and reduced graft survival. In biopsies with no rejection at all levels of stringency, TCMR activity still correlated with i- and t-lesions, molecular injury, depressed eGFR, and reduced graft survival. TCMR activity in no rejection biopsies selectively correlated with TCMR features but not with DSA, C4d, ABMR lesions, or proteinuria. Thus, in no rejection biopsies subthreshold TCMR activity remained specific for the defining features of the TCMR process.

In all biopsies, ABMR activity correlated strongly with DSA, C4d, and ptc-, g-, cg, and v-lesions and proteinuria and with graft loss (Table 2). In biopsies with no molecular or histologic rejection even when defined by maximum stringency (Level 3), subthreshold ABMR activity still correlated with DSA and histologic g-lesions and not with TCMR features, proteinuria, C4d, cg-lesions, molecular injury, or 3-year graft loss. In all levels of no

Table 1
Correlation of TCMR molecular activity ($TCMR_{Prob}$ classifier score) with conventional features in all biopsies and in biopsies with no rejection.

Feature category	Feature	All (N = 5086)		Level 1 no rejection (N = 2842 by archetypes)		Level 2 no rejection[a] (N = 2341 by archetypes and MMDx signout)		Level 3 no rejection (N = 715 by archetypes, MMDx signout, and histology)	
		Correlation[b]	*P*	Correlation	*P*	Correlation	*P*	Correlation	*P*
TCMR-related	t-lesion scores[c]	**0.46**	**$<2.2 \times e^{-16}$**	**0.29**	**$<2.2 \times e^{-16}$**	**0.27**	**$<2.2 \times e^{-16}$**	**0.12**	**.001**
	i-lesion scores[c]	**0.41**	**$<2.2 \times e^{-16}$**	**0.19**	**$9.3 \times e^{-11}$**	**0.17**	**$9.1 \times e^{-8}$**	**0.10**	**.009**
ABMR-related	DSA status[c]	0.02	.48	−0.03	.41	0.005	.90	−0.01	.80
	C4d status[c]	0.08	$2.5 \times e^{-4}$	0.04	.15	0.05	.13	0.06	.10
	g-lesion scores[c]	0.00	.98	−0.05	.063	−0.04	.16	−0.05	.17
	cg-lesion scores[c]	−0.06	.004	−0.02	.43	−9.70	1.00	0.004	.90
	ptc-lesion scores[c]	**0.17**	**$3.8 \times e^{-15}$**	0.06	.032	0.05	.15	0.06	.10
All rejection-related	v-lesion scores[c]	**0.23**	**$<2.2 \times e^{-16}$**	0.08	.005	**0.10**	**.002**	0.06	.10
Injury-related	GFR[c]	**−0.15**	**$3.0 \times e^{-16}2$**	−0.08	.009	−0.06	.06	**−0.10**	**.01**
	Proteinuria[c]	0.04	.09	0.05	.08	0.04	.17	0.07	.06
	Injury-induced transcripts (IRRAT)	**0.45**	**$<2.2 \times e^{-16}$**	**0.31**	**$<2.2 \times e^{-16}$**	**0.30**	**$<2.2 \times e^{-16}$**	**0.32**	**$<2.2 \times e^{-16}$**
	3-y survival (Cox)[c,d]	***P* = $1.7 \times e^{-5}$**		***P* = .03**		***P* = .03**		***P* = .0005**	

AA, archetypal analysis; ABMR, antibody-mediated rejection; DSA, donor-specific antibody; GFR, glomerular filtration rate; MMDx, Molecular Microscope Diagnostic System; TCMR, T cell–mediated rejection.

[a] Some NR archetype biopsies (177) were excluded because the MMDx signout was unavailable, and 324 were excluded because MMDx signouts detected rejection changes: 120 called ABMR, 13 mixed, 116 possible ABMR, 42 possible TCMR, and 33 TCMR.

[b] Spearman correlation coefficients of ≥ 0.10 or ≤ -0.10 with $ABMR_{Prob}$ and their *P* values are bolded.

[c] Values represented are within known data for these fields.

[d] Significant *P* values ($\leq$.05 log-rank test) in Cox analysis are bolded and shaded; 1 random Bx per organ, only including samples with estimated %cortex of >10; N = 1292, 210 failures within all; N = 780, 91 failures within no rejection by AA; n = 641, 71 failures for no rejection by AA and MMDx signouts.

Table 2

Correlation of ABMR molecular activity ($ABMR_{Prob}$ classifier score) with conventional features in all biopsies and in biopsies with no rejection.

Feature category	Feature	All (N = 5086)		Level 1 no rejection (N = 2842 by archetypes)		Level 2 no rejection (N = 2341 by archetypes and MMDx signout)[a]		Level 3 no rejection (N = 715 by archetypes, MMDx signout, and histology)	
		Correlation[b]	*P*	Correlation	*P*	Correlation	*P*	Correlation	*P*
TCMR-related	t-lesion scores[c]	0.08	$4.0 \times e^{-4}$	0.06	.04	0.03	.40	0.02	.50
	i-lesion scores[c]	**0.13**	**$2.1 \times e^{-9}$**	0.07	.011	0.03	.40	0.03	.40
ABMR-related	DSA status[c]	**0.37**	**$<2.2 \times e^{-16}$**	**0.21**	**$5.6 \times e^{-12}$**	**0.12**	**.0004**	**0.10**	**.02**
	C4d status[c]	**0.32**	**$<2.2 \times e^{-16}$**	0.07	.01	0.05	.12	−0.006	.90
	g-lesion scores[c]	**0.53**	**$<2.2 \times e^{-16}$**	**0.24**	**$<2.2 \times e^{-16}$**	**0.18**	**$4.8 \times e^{-9}$**	**0.14**	**.0002**
	cg-lesion scores[c]	**0.37**	**$<2.2 \times e^{-16}$**	**0.17**	**$3.0 \times e^{-9}$**	**0.11**	**.0004**	0.05	.17
	ptc-lesion scores[c]	**0.55**	**$<2.2 \times e^{-16}$**	**0.20**	**$7.3 \times e^{-12}$**	0.10	.002	0.06	.10
All rejection-related	v-lesion scores[c]	**0.17**	**$3.0 \times e^{-14}$**	0.09	.0014	0.09	.008	0.04	.30
Injury-related	eGFR[c]	0.05	.04	0.06	.04	0.09	.003	**0.12**	**.002**
	Proteinuria[c]	**0.13**	**$7.2 \times e^{-9}$**	0.02	.41	0.03	.40	0.03	.40
	Injury-associated transcripts (IRRAT)[c]	0.09	$6.1 \times e^{-11}$	0.04	.02	0.01	.70	0.03	.50
	3-y survival (Cox)[c,d]	***P* = .02**		*P* = .42		*P* = .39		*P* = .70	

ABMR, antibody-mediated rejection; eGFR, estimated glomerular filtration rate; MMDx, Molecular Microscope Diagnostic System; TCMR, T cell–mediated rejection.

[a] Some no rejection biopsies were excluded because the MMDx signout was unavailable in 177 biopsies called NR by archetypes, and 324 were excluded because MMDx signouts detected rejection changes: 120 called ABMR, 13 mixed, 116 possible ABMR, 42 possible TCMR, and 33 TCMR.

[b] Spearman correlation coefficients of ≥ 0.10 or $\leq$ -0.10 with $ABMR_{Prob}$ and their *P* values are bolded.

[d] Significant *P* values ($\leq$.05 log-rank test) in Cox analysis are bolded and shaded; 1 random Bx per organ, only including samples with estimated %cortex of >10; N = 1292, 210 failures within all; N = 780, 91 failures within NR by AA; n = 641, 71 failures within No rejection by AA and by MMDx signouts.

Table 3
Relationship between ABMR or TCMR activity in a No rejection biopsy (index biopsy) and actual molecular ABMR or TCMR diagnosed (by archetype assignment) in the next biopsy[a].

	Classifiers defining activity	Comparing the mean rejection activity scores in index biopsy with No rejection to the finding of No rejection, ABMR, or TCMR in a subsequent biopsy				
		When next biopsy shows No rejection (Level 1, N = 267; Level 2, N = 232)	When next biopsy shows ABMR (Level 1, N = 75; Level 2, N = 38)	P[b] No rejection vs ABMR	When next biopsy shows TCMR (Level 1, N = 49; Level 2, N = 36)	P[b] No rejection vs TCMR
Index biopsy Level 1[a] No rejection (N = 391 pairs)	TCMR activity ($TCMR_{Prob}$)	0.04	0.03	.38	**0.06**	**$6.9 \times e^{-4}$**
	ABMR activity ($ABMR_{Prob}$)	0.09	**0.14**[c]	**$1.2 \times e^{-9}$**	0.10	.35
Index biopsy Level 2[a] No rejection (N = 306 pairs)	TCMR activity ($TCMR_{Prob}$)	0.03	0.03	.14	**0.07**	**.04**
	ABMR activity ($ABMR_{Prob}$)	0.08	**0.11**	**$4.7 \times e^{-4}$**	0.08	.97

ABMR, antibody-mediated rejection; DSA, donor-specific antibody; GFR, glomerular filtration rate; MMDx, Molecular Microscope Diagnostic System; TCMR, T cell–mediated rejection.

[a] N = 391 No rejection Level 1 biopsies (NR by archetypes only) and N = 306 No rejection Level 2 (NR by archetypes and no rejection by MMDx sign-outs) index biopsies with rejection archetype assignments in the next follow-up biopsy. There were too few pairs in No rejection Level 3 to analyze.

[b] P values determined by Wilcoxon test (1-tailed when a result is expected, ie, an increase in $ABMR_{Prob}$ in ABMR, or $TCMR_{Prob}$ in TCMR and 2-tailed otherwise), comparing scores within the index case no rejection biopsies with those that went on to be No rejection vs ABMR vs TCMR in the next biopsy.

[c] Bolding indicates values where the corresponding P value was significant (<.05).

rejection biopsies, neither ABMR nor TCMR correlated significantly with ptc-lesions, suggesting that very low levels of ptc-lesions can be induced by other injuries.

In summary, when rejection was rigorously excluded by histologic and molecular criteria, subthreshold TCMR and ABMR activity was not nonspecific but had mutually exclusive selective associations with defining conventional and molecular features: TCMR activity with subthreshold i- and t-lesions, molecular injury, decreased eGFR, and decreased graft survival and ABMR activity with DSA and subthreshold g-lesions.

3.6. Subthreshold rejection activity in no rejection biopsies anticipates more actual rejection in future biopsies

Some patients in the 5086 biopsy cohort underwent a later biopsy as standard-of-care. We examined the 391 biopsy pairs in which the first biopsy (index biopsy) had no rejection and a second biopsy (follow-up biopsy) was performed later (inclusion criteria for this subpopulation was that a follow-up biopsy had to be available within our data set and the first biopsy of the pair had to be called NR at minimum by the archetypal analysis, and we added 2 more levels of stringency). In each pair, we studied whether molecular ABMR or TCMR diagnoses in the later biopsy was anticipated by higher ABMR or TCMR activity scores, respectively, in the preceding index biopsy designated as no rejection (Table 3). We defined no rejection in the index biopsy by Level 1 or Level 2 stringency; there were too few pairs at Level 3 stringency for reliable assessments.

When the follow-up biopsy had ABMR, the preceding no rejection index biopsy had higher ABMR activity than when the follow-up biopsy had NR or TCMR. Similarly, when the follow-up biopsy had TCMR, the preceding index no rejection biopsy had higher TCMR activity than when the follow-up biopsy had no rejection or ABMR. This was seen at both Level 1 and Level 2 stringency of the no rejection definition.

Therefore, increased subthreshold rejection activity in biopsies classified as no rejection anticipates a higher probability that actual rejection will be diagnosed in future standard-of-care biopsies: ABMR activity anticipates actual ABMR but not TCMR, and TCMR activity anticipates actual TCMR but not ABMR.

4. Discussion

Standardized processing of 5086 biopsies, mostly for indications, provided us with an opportunity to study the relationship between gradients of TCMR and ABMR molecular activity in biopsies currently classified as no rejection and various clinical, histologic, and molecular features. To ensure that we captured as much actual rejection as possible, we developed a new more rigorous 7-archetype model that designated a lower fraction of

the biopsies as archetypal NR (56%) compared with 62% in earlier analyses,[14] based on automatically assigned archetype groups. The new classification recognized a Minor ABMR class at the boundary between rejection and NR. While archetypal clustering assigned rejection groups, PCA and UMAP showed continuous distributions, questioning the concept of rejection states as dichotomous. Subthreshold molecular rejection activity, defined by the $TCMR_{Prob}$ and $ABMR_{Prob}$ classifiers, was extensive in many biopsies classified as NR but remained specific for the defining features of TCMR and ABMR respectively, selectively correlating with the histologic, clinical, and molecular features. In addition, there was subthreshold TCMR activity in many ABMR biopsies and subthreshold ABMR activity in many TCMR biopsies. We conclude that, unlike our previous concept of ABMR and TCMR as largely dichotomous classes, the 2 effector arms of the host adaptive immune response generate activity gradients with considerable subthreshold activity that has not been previously appreciated.

The associations of subthreshold molecular ABMR and TCMR activity with low levels of the histology and clinical features that define these conditions confirm that these two gradients remain distinct and specific even at the subthreshold levels. Even after excluding all biopsies diagnosed molecularly or histologically as rejection or possible rejection, TCMR activity still strongly correlated with the subthreshold scores for the defining features of TCMR—tubulitis, interstitial infiltration, molecular injury, depressed eGFR, and increased graft loss, but not with ABMR-related features; ABMR activity correlated with 2 defining features of ABMR—DSA and g-lesions, and not with TCMR features. The specificity and clinical relevance of the subthreshold activity were apparent in the index biopsy–future biopsy analysis, where subthreshold TCMR or ABMR activity in biopsies with no rejection anticipated a higher probability that a future indication biopsy will have actual TCMR or ABMR, respectively.

The finding that TCMR and ABMR activity operates as gradients affecting the majority of biopsies should not be surprising when we consider that every organ transplant recipient can mount allospecific T cell and B cell responses. The ISDs that make organ transplantation possible were developed for suppressing clinical rejection episodes, not for preventing all adaptive immune activity. Our previous histologic and molecular approaches to rejection imposed dichotomous classes on continuous distributions but now must acknowledge that these classes represent the high end of gradients.

ABMR and TCMR activity in biopsies currently considered no rejection should not be construed as an indication to treat but rather a challenge to develop new evidence on the impact of treatment. In responding to subthreshold rejection activity, we must appreciate that management of both TCMR and ABMR is inadequate, as illustrated in the survival analysis in Figure 3. The high frequency of graft loss following biopsy-diagnosed TCMR contradicts the belief that TCMR is treatable: TCMR1 and TCMR2 outcomes were similar to FABMR and LABMR, which are considered resistant to treatment.[26] The focus must not be on treating subthreshold rejection gradients but on optimizing the treatment of actual TCMR and ABMR and then evaluating these effective interventions in the subthreshold states. In addition, the fact that TCMR1 and TCMR2 had less than expected afferent arteriolar hyalinosis reminds us to reemphasize the maintenance of therapeutic levels of immunosuppression and prevent nonadherence.

On a population-wide basis, ABMR causes microcirculation stress that can be relatively well-tolerated for long periods as subthreshold, Minor ABMR, and EABMR before progressing to proteinuria, declining GFR, and impaired survival. While subthreshold ABMR and Minor ABMR do not significantly impact 3-year survival, their similarity to the more active states suggests that many will eventually progress albeit over a longer period that cannot be captured in a cross-sectional study such as this. (Note that the slight increase in 3-year graft loss with subthreshold ABMR observed in our earlier study of no rejection biopsies[14] is not observed in the new more rigorous definition, probably because the new system reclassified some previous no rejection as ABMR.)

Despite the advantages of large numbers of biopsies from the international kidney transplant population assessed by standardized algorithms, this study has limitations imposed by its cross-sectional observational design. Moreover, the conclusions only apply to biopsied patients: the frequency of subthreshold TCMR or ABMR activity in patients never having biopsies is unknown. We also acknowledge that imposing artificial classes on continuous distributions must create errors in cases near boundaries.

Subthreshold rejection states can probably be detected using noninvasive monitoring: elevated dd-cfDNA is found in patients without biopsy indications, potentially representing smoldering rejection activity in many persons with biopsies read as no rejection.[27-29] Our findings in the Trifecta-Kidney study indicate that subthreshold ABMR activity probably explains at least some dd-cfDNA elevation in biopsies classified as no rejection.[21,29] Subthreshold ABMR activity in no rejection biopsies did not trigger proteinuria or depress eGFR, and DSA negativity is common in subthreshold ABMR. Ideally, we should monitor the cognate host alloimmune activity directly, but these methods are imperfect. T cell reactivity is rarely directly assessed, although proposed technologies for this are in development.[30-36]

Our findings emphasize close relationships between molecular changes and histologic lesions, suggesting that detection of subthreshold rejection activity by histology should be possible. A new look at how to detect subthreshold TCMR and ABMR by histology features is warranted, guided by molecular gradients of rejection-associated activity. As the availability of effective therapies expands, our understanding of increased subclinical rejection activity should prompt closer monitoring in those patients (potentially through noninvasive testing, eg, dd-cfDNA, or closer monitoring of clinical variables, eg, GFR or proteinuria). This could provide clinicians with a clearer picture of the patient's rejection trajectory and better clinical context for effective patient management of either ABMR or TCMR.

Acknowledgments

The authors thank their valued clinicians in the INTERCOMEX and Trifecta study groups who partnered with them for this study by contributing biopsies, data, and feedback.

Funding

This research has been principally supported by grants from Genome Canada, Canada Foundation for Innovation, the University of Alberta Hospital Foundation, the Alberta Ministry of Advanced Education, the Mendez National Institute of Transplantation Foundation, and Industrial Research Assistance Program. Partial support was also provided by funding from a licensing agreement with the One Lambda division of ThermoFisher. The Trifecta study is an investigator-initiated study supported by a grant from Natera to Transcriptome Sciences/ATAGC. The MMDx project is supported in part by a licensing agreement with One Lambda Inc./Thermo Fisher Scientific.

Declaration of competing interest

The authors of this manuscript have conflicts of interest to disclose as described by the *American Journal of Transplantation*. P.F. Halloran holds shares in Transcriptome Sciences Inc., a University of Alberta research company dedicated to developing molecular diagnostics, supported in part by a licensing agreement between Transcriptome Sciences Inc. and Thermo Fisher Scientific, and by a research grant from Natera, Inc. P.F. Halloran is a consultant to Natera, Inc. and Argenx BV. The other authors have declared no conflict of interest exists.

Data availability

The CEL files are available on the Gene Expression Omnibus website (GSE275126).

Appendix A. Supplementary data

Supplementary data to this article can be found online at https://doi.org/10.1016/j.ajt.2024.07.034.

ORCiD

Philip F. Halloran https://orcid.org/0000-0003-1371-1947
Katelynn S. Madill-Thomsen https://orcid.org/0000-0003-2781-6934
Georg Böhmig https://orcid.org/0000-0002-7600-912X
Klemens Budde https://orcid.org/0000-0002-7929-5942
Meagan Barner https://orcid.org/0000-0002-8723-7136
Martina Mackova https://orcid.org/0009-0006-7822-5746
Jessica Chang https://orcid.org/0000-0001-5039-2186
Gunilla Einecke https://orcid.org/0000-0003-0205-9068
Farsad Eskandary https://orcid.org/0000-0002-8971-6149
Gaurav Gupta https://orcid.org/0000-0003-1919-1970
Marek Myślak https://orcid.org/0000-0002-9569-031X
Ondrej Viklicky https://orcid.org/0000-0003-1049-2195
Enver Akalin https://orcid.org/0000-0003-1341-5144
Tarek Alhamad https://orcid.org/0000-0003-4289-0817
Miha Arnol https://orcid.org/0000-0002-2379-7820
Mirosław Banasik https://orcid.org/0000-0002-0588-1551
Adam Bingaman https://orcid.org/0000-0001-5521-8187
Christopher D. Blosser https://orcid.org/0000-0001-8368-6682
Daniel Brennan https://orcid.org/0000-0002-4818-7455
Andrzej Chamienia https://orcid.org/0000-0002-9213-4801
Michał Ciszek https://orcid.org/0000-0003-0641-5920
Declan de Freitas https://orcid.org/0009-0001-9197-3443
Dominika Dęborska-Materkowska https://orcid.org/0000-0002-7282-0177
Alicja Debska-Ślizień https://orcid.org/0000-0001-8210-8063
Arjang Djamali https://orcid.org/0000-0001-7675-6128
Leszek Domański https://orcid.org/0000-0002-4712-7821
Magdalena Durlik https://orcid.org/0000-0002-4798-1497
Richard Fatica https://orcid.org/0000-0003-2455-641X
Justyna Fryc https://orcid.org/0000-0002-7895-1012
John Gill https://orcid.org/0000-0002-8837-6875
Jagbir Gill https://orcid.org/0000-0001-8072-265X
Maciej Glyda https://orcid.org/0000-0002-0566-870X
Sita Gourishankar https://orcid.org/0000-0002-6442-895X
Ryszard Grenda https://orcid.org/0000-0002-6814-6589
Petra Hruba https://orcid.org/0000-0002-8663-413X
Peter Hughes https://orcid.org/0009-0004-7659-0585
Arskarapurk Jittirat https://orcid.org/0009-0003-9215-5674
Zeljka Jurekovic https://orcid.org/0000-0003-0690-2577
Layla Kamal https://orcid.org/0000-0002-3797-5544
Sam Kant https://orcid.org/0000-0001-5863-3562
Bertram Kasiske https://orcid.org/0000-0003-4809-6956
Nika Kojc https://orcid.org/0000-0003-1893-4349
Roslyn Mannon https://orcid.org/0000-0003-1776-3680
Arthur Matas https://orcid.org/0000-0001-9957-639X
Joanna Mazurkiewicz https://orcid.org/0000-0003-3560-3402
Marius Miglinas https://orcid.org/0000-0002-0017-468X
Seth Narins https://orcid.org/0000-0002-3888-0424
Beata Naumnik https://orcid.org/0000-0001-7090-8856
Anita Patel https://orcid.org/0000-0003-0359-1929
Agnieszka Perkowska-Ptasińska https://orcid.org/0000-0001-5524-3534
Michael Picton https://orcid.org/0000-0002-3066-0638
Grzegorz Piecha https://orcid.org/0000-0001-8371-0195
Emilio Poggio https://orcid.org/0000-0003-1492-5103
Silvie Rajnochová Bloudíčkova https://orcid.org/0000-0003-0270-571X
Milagros Samaniego-Picota https://orcid.org/0000-0001-7914-1663
Thomas Schachtner https://orcid.org/0000-0001-5549-4798
Soroush Shojai https://orcid.org/0000-0002-2969-9121
Majid L.N. Sikosana https://orcid.org/0000-0001-9477-432X
Janka Slatinská https://orcid.org/0000-0001-5095-8338
Katarzyna Smykal-Jankowiak https://orcid.org/0009-0001-7091-7215
Željka Veceric Haler https://orcid.org/0000-0003-3318-9850
Ksenija Vucur https://orcid.org/0000-0002-8255-4933
Matthew R. Weir https://orcid.org/0000-0001-8820-5702
Andrzej Wiecek https://orcid.org/0000-0002-8625-4188
Harold Yang https://orcid.org/0009-0003-5541-6310
Ziad Zaky https://orcid.org/0000-0001-9752-0050

References

1. Hariharan S, Israni AK, Danovitch G. Long-term survival after kidney transplantation. *N Engl J Med*. 2021;385(8):729–743. https://doi.org/10.1056/NEJMra2014530.
2. Halloran PF. Immunosuppressive drugs for kidney transplantation. *N Engl J Med*. 2004;351(26):2715–2729. https://doi.org/10.1056/NEJMra033540.
3. Ekberg H, Tedesco-Silva H, Demirbas A, et al. Reduced exposure to calcineurin inhibitors in renal transplantation. *N Engl J Med*. 2007;357(25):2562–2575. https://doi.org/10.1056/NEJMoa067411.

4. Naesens M, Roufosse C, Haas M, et al. The Banff 2022 Kidney Meeting Report: reappraisal of microvascular inflammation and the role of biopsy-based transcript diagnostics. *Am J Transplant*. 2024;24(3):338–349. https://doi.org/10.1016/j.ajt.2023.10.016.
5. Tambur AR, Campbell P, Claas FH, et al. Sensitization in Transplantation: assessment of Risk (STAR) 2017 working group meeting report. *Am J Transplant*. 2018;18(7):1604–1614. https://doi.org/10.1111/ajt.14752.
6. Reed EF, Rao P, Zhang Z, et al. Comprehensive assessment and standardization of solid phase multiplex-bead arrays for the detection of antibodies to HLA. *Am J Transplant*. 2013;13(7):1859–1870. https://doi.org/10.1111/ajt.12287.
7. Xiao H, Gao F, Pang Q, et al. Diagnostic accuracy of donor-derived cell-free DNA in renal-allograft rejection: a meta-analysis. *Transplantation*. 2021;105(6):1303–1310. https://doi.org/10.1097/TP.0000000000003443.
8. Halloran PF, Madill-Thomsen KS, Reeve J. The molecular phenotype of kidney transplants: insights from the MMDx project. *Transplantation*. 2024;108(1):45–71. https://doi.org/10.1097/TP.0000000000004624.
9. Halloran PF, Madill-Thomsen KS. The Molecular Microscope Diagnostic System: assessment of rejection and injury in heart transplant biopsies. *Transplantation*. 2023;107(1):27–44. https://doi.org/10.1097/TP.0000000000004323.
10. Halloran PF, Bohmig GA, Bromberg J, et al. Archetypal analysis of injury in kidney transplant biopsies identifies two classes of early AKI. *Front Med (Lausanne)*. 2022;9:817324. https://doi.org/10.3389/fmed.2022.817324.
11. Madill-Thomsen KS, Bohmig GA, Bromberg J, et al. Relating molecular T cell-mediated rejection activity in kidney transplant biopsies to time and to histologic tubulitis and atrophy-fibrosis. *Transplantation*. 2023;107(5):1102–1114. https://doi.org/10.1097/TP.0000000000004396.
12. Bohmig GA, Halloran PF, Feucht HE. On a long and winding road: alloantibodies in organ transplantation. *Transplantation*. 2023;107(5):1027–1041. https://doi.org/10.1097/TP.0000000000004550.
13. Halloran PF, Madill-Thomsen KS, Pon S, et al. Molecular diagnosis of ABMR with or without donor-specific antibody in kidney transplant biopsies: differences in timing and intensity but similar mechanisms and outcomes. *Am J Transplant*. 2022;22(8):1976–1991. https://doi.org/10.1111/ajt.17092.
14. Madill-Thomsen KS, Bohmig GA, Bromberg J, et al. Donor-specific antibody is associated with increased expression of rejection transcripts in renal transplant biopsies classified as no rejection. *J Am Soc Nephrol*. 2021;32(11):2743–2758. https://doi.org/10.1681/ASN.2021040433.
15. Rosales IA, Mahowald GK, Tomaszewski K, et al. Banff human organ transplant transcripts correlate with renal allograft pathology and outcome: importance of capillaritis and subpathologic rejection. *J Am Soc Nephrol*. 2022;33(12):2306–2319. https://doi.org/10.1681/ASN.2022040444.
16. Halloran PF, Pereira AB, Chang J, et al. Potential impact of microarray diagnosis of T cell-mediated rejection in kidney transplants: the INTERCOM study. *Am J Transplant*. 2013;13(9):2352–2363. https://doi.org/10.1111/ajt.12387. In File.
17. Halloran PF, Pereira AB, Chang J, et al. Microarray diagnosis of antibody-mediated rejection in kidney transplant biopsies: an international prospective study (INTERCOM). *Am J Transplant*. 2013;13(11):2865–2874. https://doi.org/10.1111/ajt.12465.
18. Reeve J, Bohmig GA, Eskandary F, et al. Generating automated kidney transplant biopsy reports combining molecular measurements with ensembles of machine learning classifiers. *Am J Transplant*. 2019;19(10):2719–2731. https://doi.org/10.1111/ajt.15351.
19. Halloran PF, Reeve J, Akalin E, et al. Real time central assessment of kidney transplant indication biopsies by microarrays: the INTERCOMEX study. *Am J Transplant*. 2017;17(11):2851–2862. https://doi.org/10.1111/ajt.14329.
20. Reeve J, Bohmig GA, Eskandary F, et al. Assessing rejection-related disease in kidney transplant biopsies based on archetypal analysis of molecular phenotypes. *JCI Insight*. 2017;2(12):e94197. https://doi.org/10.1172/jci.insight.94197.
21. Halloran PF, Reeve J, Madill-Thomsen KS, et al. The Trifecta Study: comparing plasma levels of donor-derived cell-free DNA with the molecular phenotype of kidney transplant biopsies. *J Am Soc Nephrol*. 2022;33(2):387–400. https://doi.org/10.1681/ASN.2021091191.
22. Halloran PF, Reeve J, Madill-Thomsen KS, et al. Combining donor-derived cell-free DNA fraction and quantity to detect kidney transplant rejection using molecular diagnoses and histology as confirmation. *Transplantation*. 2022;106(12):2435–2442. https://doi.org/10.1097/TP.0000000000004212.
23. Halloran PF, Reeve J, Madill-Thomsen KS, et al. Antibody-mediated rejection without detectable donor-specific antibody releases donor-derived cell-free DNA: results from the Trifecta study. *Transplantation*. 2023;107(3):709–719.
24. R Core Team. *R: A language and environment for statistical computing*. R Foundation for statistical Computing; 2019. Updated http://www.r-project.org/.
25. Famulski KS, de Freitas DG, Kreepala C, et al. Molecular phenotypes of acute kidney injury in kidney transplants. *J Am Soc Nephrol*. 2012;23(5):948–958. https://doi.org/10.1681/ASN.2011090887.
26. Bohmig GA, Eskandary F, Doberer K, Halloran PF. The therapeutic challenge of late antibody-mediated kidney allograft rejection. *Transpl Int*. 2019;32(8):775–788. https://doi.org/10.1111/tri.13436.
27. Filippone EJ, Farber JL. The monitoring of donor-derived cell-free DNA in kidney transplantation. *Transplantation*. 2021;105(3):509–516. https://doi.org/10.1097/TP.0000000000003393.
28. Kataria A, Kumar D, Gupta G. Donor-derived cell-free DNA in solid-organ transplant diagnostics: indications, limitations, and future directions. *Transplantation*. 2021;105(6):1203–1211. https://doi.org/10.1097/TP.0000000000003651.
29. Gauthier PT, Madill-Thomsen KS, Demko Z, et al. Distinct molecular processes mediate donor-derived cell-free DNA release from kidney transplants in different disease states. *Transplantation*. 2024;108(4):898–910. https://doi.org/10.1097/TP.0000000000004877.
30. Spitznagel T, Matter LS, Kaufmann YL, Nilsson J, von Moos S, Schachtner T. PIRCHE-II scores prove useful as a predictive biomarker among kidney transplant recipients with rejection: an analysis of indication and follow-up biopsies. *Front Immunol*. 2022;13:949933. https://doi.org/10.3389/fimmu.2022.949933.
31. Niemann M, Matern BM, Spierings E. Snowflake: a deep learning-based human leukocyte antigen matching algorithm considering allele-specific surface accessibility. *Front Immunol*. 2022;13:937587. https://doi.org/10.3389/fimmu.2022.937587.
32. Otten HG, Calis JJ, Kesmir C, van Zuilen AD, Spierings E. Predicted indirectly recognizable HLA epitopes presented by HLA-DR correlate with the de novo development of donor-specific HLA IgG antibodies after kidney transplantation. *Hum Immunol*. 2013;74(3):290–296. https://doi.org/10.1016/j.humimm.2012.12.004.
33. Lachmann N, Niemann M, Reinke P, et al. Donor-recipient matching based on predicted indirectly recognizable HLA epitopes independently predicts the incidence of de novo donor-specific HLA antibodies following renal transplantation. *Am J Transplant*. 2017;17(12):3076–3086. https://doi.org/10.1111/ajt.14393.
34. Niemann M, Lachmann N, Geneugelijk K, Spierings E. Computational Eurotransplant kidney allocation simulations demonstrate the feasibility and benefit of T-cell epitope matching. *PLOS Comput Biol*. 2021;17(7):e1009248. https://doi.org/10.1371/journal.pcbi.1009248.

35. Niemann M, Strehler Y, Lachmann N, et al. Snowflake epitope matching correlates with child-specific antibodies during pregnancy and donor-specific antibodies after kidney transplantation. *Front Immunol*. 2022;13: 1005601. https://doi.org/10.3389/fimmu.2022.1005601.
36. Senev A, Lerut E, Coemans M, et al. Association of HLA mismatches and histology suggestive of antibody-mediated injury in the absence of donor-specific anti-HLA antibodies. *Clin J Am Soc Nephrol*. 2022;17(8): 1204–1215. https://doi.org/10.2215/CJN.00570122.
37. Wood SN. *Generalized Additive Models*. 2nd Edition. Boca Raton: Chapman and Hall/CRC; 2017.
38. Harrell FE. *Regression modelling strategies with applications to linear models, logistic regression and survival analysis*. New York: Springer; 2001.